

# Iron chelator-induced growth arrest and cytochrome c-dependent apoptosis in immortalized and malignant oral keratinocytes

Sun-Kyung Lee<sup>1</sup>, Jae-Jung Lee<sup>1</sup>, Hwa-Jeong Lee<sup>1</sup>, Jun Lee<sup>2</sup>, Byung-Hun Jeon<sup>3</sup>, Chang-Duk Jun<sup>4</sup>, Suk-Keun Lee<sup>5</sup>, Eun-Cheol Kim<sup>1</sup>

<sup>1</sup>Department of Oral and Maxillofacial Pathology, <sup>2</sup>Department of Oral and Maxillofacial Surgery, College of Dentistry, <sup>3</sup>Department of Pathology, College of Oriental Medicine, Wonkwang University, Iksan, Korea; <sup>4</sup>Department of Life Science, Gwangju Institute of Science and Technology, Gwangju, Korea; <sup>5</sup>Department of Oral Pathology, College of Dentistry, Kangnung National University, Gangneung, Korea

**BACKGROUND:** Many studies have shown the anti-proliferative effects of iron deprivation on cancer cells, but the effects of iron-chelators on oral cancer have not been clearly elucidated.

**METHODS:** To investigate the effects of an iron chelator, desferrioxamine (DFO), on the growth of immortalized human oral keratinocytes (IHOK), primary oral cancer cells (HN4), metastatic oral cancer cells (HN12) and human skin keratinocytes (HaCaT) in the MTT assay, three-dimensional (3D) raft cultures, Western blotting, cell cycle analysis, nuclear staining and cytochrome c expression for apoptosis signaling pathway were used.

**RESULTS:** Desferrioxamine inhibited the growth of immortalized IHOK and HaCaT and malignant HN4 and HN12 keratinocytes in a time- and dose-dependent manner according to the MTT assay. The 3D organotypic culture also revealed that DFO-treated cells showed less epithelial maturation, less surface keratinization and decreased epithelial thickness. The major mechanism of growth inhibition with the micromolar DFO treatment was by the induction of apoptosis, which was supported by nuclear DAPI staining, DNA fragmentation analysis and flow cytometric analysis for sub-G<sub>1</sub> phase arrest and Annexin V-FITC (fluorescein isothiocyanate) staining. Furthermore, Bax expression increased together with p53 and p21<sup>WAF1/CIP1</sup>, while the Bcl-2 expression decreased in the immortalized and malignant keratinocytes treated with DFO. Time-dependent cytochrome c from mitochondria was observed in DFO-treated IHOK and oral cancer cells and was accompanied by the activation of caspase-3 in IHOK cells.

**CONCLUSION:** These results demonstrate that DFO has growth inhibitory effects on immortalized and malignant oral keratinocytes through the induction of apoptosis and suggest that further evaluation of DFO as a potential therapeutic agent for human oral precancerous lesions is warranted.

*J Oral Pathol Med* (2006) 35: 218–26

**Keywords:** apoptosis; cell cycle; growth; IHOK; iron chelator; oral cancer cells

## Introduction

Oral squamous cell carcinoma (SCC) is the most common malignant neoplasm of the oral cavity and tends to be aggressive if not discovered early. Although the treatment methods for oral cancer have improved, the survival rates for patients with oral SCC have increased only slightly over the last few decades (1, 2). Several regimens of chemotherapy have been clinically applied for the treatment of SCC but have turned out to be insufficient at improving the prognosis (3, 4). Furthermore, the toxic effects of chemotherapy, regardless of the malignancy being treated, are always unpleasant and often cause serious complications. Therefore, alternative strategies with minimal or no side-effects should be carefully considered for the management of oral cancers.

Iron has a role not only in the synthesis of hemoglobin but also in cell growth, including tumor development and progression. Excess iron aids tumor development by catalyzing the production of oxygen radicals that may be proximate carcinogens and by being a limiting nutrient to the growth and replication of cancer cells (5, 6). Tumor growth is enhanced by iron as observed in cell culture (7) and in animal (8, 9) and human studies (10–13). Many tumors readily take up

Correspondence: Eun-Cheol Kim DDS PhD, Department of Oral and Maxillofacial Pathology, Dental College, Wonkwang University, Shinyoungdong 344-2, Iksan City, Jeonbuk, 570-749, South Korea. Tel.: +82 63 850 6929. Fax: +82 63 850 7313. E-mail: eckwkop@wonkwang.ac.kr

Accepted for publication December 15, 2005

iron as seen by the higher iron contents found in many premalignant and malignant tissues compared with that in normal tissue (14, 15).

Based on the probable role of iron in tumor development, iron withdrawal strategies have been investigated in the management of human tumors (16, 17). Iron chelators have been shown to inhibit the growth and/or induce the apoptosis of malignant cell lines from leukemia, neuroblastoma, melanoma, hepatoma, Kaposi's sarcoma and cervical cancer (18–23).

To our knowledge, iron chelating agents manifesting anti-oral cancer effects has not been reported so far and there are no comparative studies on the effects of desferrioxamine (DFO) on skin keratinocytes vs. oral keratinocytes and on immortalized cells vs. oral cancer cells. In this study, we demonstrated that DFO causes growth inhibition of human skin keratinocytes (HaCaT), oral immortalized keratinocytes (IHOK) and oral SCC cell lines (HN4 and HN12) primarily by inducing apoptotic cell death.

## Materials and methods

### Reagents

Six-well tissue culture plates and plastic Petri dishes were purchased from Falcon (Franklin Lakes, NJ, USA). Dulbeccos modified Eagle's medium (DMEM), keratinocyte growth medium (KGM) medium (Clonetics), fetal bovine serum (FBS) and other tissue culture reagents were purchased from Gibco BRL (Grand Island, NY, USA). Anti-p16, p21, p53, pRb antibody were purchased from Santa Cruz (CA, USA). DFO and all other chemicals were obtained from Sigma Chemical Co. (St Louis, MO, USA) unless indicated otherwise.

### Cell culture

HPV-immortalized human oral keratinocytes (IHOK) were derived by transfecting normal human gingival epithelial cells with PLXSN vector containing the E6/E7 open reading frames of HPV type 16, following methods previously described (24). Stably transfected cells were selected using G418. The immortalized oral keratinocytes were cultured in the KGM (Gibco) supplemented with 2 ml of bovine pituitary extract (13 mg/ml), 0.5 ml each of hydrocortisone (0.5 mg/ml), human epidermal growth factor (0.5 µg/ml), insulin (5 mg/ml), epinephrine (0.5 mg/ml), transferrin (10 mg/ml), triiodothyronine (6.5 µg/ml) and GA-1000 and 0.05 mM CaCl<sub>2</sub>.

The HaCaT, HN4 (=HNSCC4) and HN12 (=HNSCC12) cells were cultured in DMEM (Biofluid, Rockville, MD, USA) containing 10% FBS (Gibco) with 100 U/ml penicillin and 100 U/ml streptomycin (Life Technologies, Gaithersburg, MD, USA). Although HaCaT cells are immortalized and are genetically abnormal (25), they retain many features of keratinocyte differentiation and represent a skin keratinocyte model. Cell line HN4 from a primary T<sub>3</sub>N<sub>0</sub>M<sub>0</sub> carcinoma of the mouth floor and HN12 from metastatic carcinoma of the oral cavity (26) were derived in the laboratory of Dr John F. Ensley (Wayne State University). All the cell lines were grown at 37°C in a humidified atmosphere of

5% CO<sub>2</sub> and 95% air. Cells were dissociated with 0.25% trypsin just before transfer for experiments and were counted using a hemocytometer.

### MTT assay

Viable cells were detected using MTT dye, which forms blue formazan crystals that are reduced by mitochondrial dehydrogenase present in living cells. Briefly,  $2 \times 10^4$  cells were seeded in a 96-well plate and cultured overnight for cell attachment. Serial dilutions of DFO added and cells were treated for 1, 3 and 5 days. After treatment, 50 µl of MTT solution [2 mg/ml in phosphate buffered saline (PBS)] were added to each well and incubated for 4 h. The plates were then centrifuged at 200 g for 10 min and the supernatant was discarded. To each well, 50 µl of DMSO were added. The plates were then shaken until the crystals had dissolved. Reduced MTT was then measured spectrophotometrically in a dual beam microtiter plate reader at 570 nm. The DFO concentration required to inhibit cell growth by 50% (IC<sub>50</sub>) was determined by interpolating the dose-response curves.

### Raft culture of keratinocytes with DFO treatment

Collagen gels for a dermal equivalent were prepared as previously described (27) using type I collagen (Nitta Gelatin, Osaka, Japan). Confluent monolayer cells were trypsinized using 0.5% trypsin/EDTA (Gibco) and recultured on a freshly prepared gel containing type I collagen and primary cultured human gingival fibroblast matrix. The gel was kept submerged in a Millicell (Becton Dickinson, Mountain View, CA, USA) for 7 days and fed every 24 h. Then, the gel was lifted to the liquid/air interface in order to supply the nutrient vertically from bottom to top and to induce keratinocyte differentiation mimicking a stratified epithelium. The raft culture was performed with DFO treatment for 7 days and the organotypic tissue was fixed entirely in 10% buffered formalin, sectioned in 4 µm thicknesses and stained for microscopic analysis and photography.

### Flow cytometric analysis

#### Propidium iodide staining

Cells ( $5 \times 10^5$ ) were cultured with or without DFO in medium containing 10% FBS in culture dishes at 37°C for 3 days. Cells were harvested, washed with PBS, fixed with 75% ethanol at 4°C for 2 h, then treated with 0.25 mg/ml of RNase A (Sigma Chemical Co.) at 37°C for 1 h. After having been washed, the cells were stained with 500 µg/ml propidium iodide (PI; Sigma Chemical Co.) at room temperature for 10 min. Analysis was performed on flow cytometer (Beckton-Dickson, Franklin Lakes, NJ, USA). The percentage of cell in each stage of the cell cycle was determined by using the cell fit analysis program on the staining profile of viable cells.

#### FITC-Annexin V and propidium iodide double staining

After dispensing with  $1 \times 10^5$  on the six-well plate and treating each trial group with the reagents, cell pellet was prepared in FACStar tube with Annexin V-FITC solution and cultured at 37°C in CO<sub>2</sub> incubator for

about 10 min. Then, PI (without NP-40; Sigma) solution was added and the ratio of cell group positive to PI/Annexin V was measured with flow cytometer (Beckton-Dickson).

#### *Morphological analysis of apoptosis by staining with DAPI*

To confirm apoptosis by morphological observation, the cells were labeled with 2 µg/ml of the DNA dye DAPI (Sigma) for 30 min at 37°C and visualized on a fluorescence microscope (Olympus, Tokyo, Japan). DAPI permeates the plasma membrane and yields blue chromatin. Viable cells display normal nuclear size and blue fluorescence, whereas apoptotic cells show condensed chromatin and fragmented nuclei.

#### *Detection of DNA fragmentation by gel electrophoresis*

Cell pellets ( $3 \times 10^6$  cells) were resuspended in 500 µl of lysis buffer (0.5% Triton X-100, 10 mM EDTA and 10 mM Tris-HCl, pH 8.0) at room temperature for 15 min and centrifuged at 16 000 *g* for 10 min. DNA was then extracted using a Wizard genomic DNA purification kit (Promega, Madison, WI, USA), precipitated with ethanol and resuspended in Tris/EDTA buffer (10 mM Tris-HCl, pH 8.0 and 1 mM EDTA). DNA was analyzed after separation by gel electrophoresis (2% agarose).

#### *Western blot analysis*

Protein samples (50 µg) were mixed with an equal volume of 2× sodium dodecyl sulfate (SDS) sample buffer, boiled for 5 min and then separated using 8–15% SDS-polyacrylamide gel electrophoresis (PAGE). After electrophoresis, the proteins were transferred to nylon membranes using electrophoretic transfer. The membranes were blocked in 5% dry milk (1 h), rinsed and incubated with secondary and primary antibodies (diluted 1:500 to 1:1000) in TBS for 1 h at room temperature. Finally, each protein was detected using an enhanced chemiluminescence system (Amersham Pharmacia Biotech, Arlington, IL, USA).

#### *Assays for caspase activities*

Caspase-3 like activities were measured by colorimetric assay using the peptide-based substrates Ac-DEVD-pNA and Ac-IETD-pNA, according to the manufacturer's recommendations (Calbiochem-Behring, La Jolla, CA, USA). At specific times after treatment with the different agents, cells were collected by scraping into cold PBS, centrifuged and lysed on ice for 10 min in the cell lysis buffer that was provided in the caspase-3 assay kit. The extracts were then reacted with the colorimetric caspase substrates (Ac-DEVD-pNA or Ac-IETD-pNA), incubated at 37°C and color changes were analyzed with a 96-well microplate spectrophotometer (Molecular Devices, Menlo Park, CA, USA) at 10 min intervals during the 3 h incubation.

#### *Evaluation of cytochrome c release from mitochondria*

At designated time-points following exposure to experimental treatments, cells [ $1 \times 10^7$ ] were trypsinized and

then washed with ice-cold buffer A (250 mM sucrose, 20 mM HEPES-KOH (pH 7.4), 1 mM EDTA, 1 mM EGTA, 2 mg/ml leupeptin, 1 mg/ml pepstatin]. The cells were resuspended in 200 ml of buffer A and carefully homogenized using a homogenizer. The homogenates were separated into cytosol (supernatant) and mitochondrial fractions (pellet) by differential centrifugation. Cytosolic and mitochondrial proteins were then subjected to immunoblot analysis using the anti-cytochrome *c* monoclonal antibody, as described above.

## Results

### *Effects of DFO on cell proliferation*

In order to compare the effects of DFO on the growth of skin (HaCaT) and oral immortalized keratinocytes (IHOK) cells, exponentially growing cells were treated with DFO and cell viability was evaluated by the MTT assay. The growth of HaCaT and IHOK cells was inhibited in a dose- and time-dependent fashion at DFO concentrations ranging from 0.1–2 mM on the days 1, 2 and 3 of culture (Fig. 1a,b). However, the IHOK cells were more sensitive to DFO than the HaCaT cells.

We next investigated the effects of DFO on the growth of HN4 (primary) and HN12 (metastatic) oral cancer cells and compared the effects to those observed with IHOK cells. The HN4 and HN12 cells also showed growth inhibition in the presence of DFO. However, these cancer cells appeared to be less sensitive to DFO than the immortalized keratinocytes (HaCaT and IHOK). Comparing the primary (HN4) and metastatic (HN12) cancer cells, the HN12 cells were more resistant to DFO than the HN4 cells.

The concentration of DFO causing 50% inhibition of cell growth ( $IC_{50}$ ) was calculated after 1, 2 and 3 days of exposure (Table 1). The  $IC_{50}$  values of the HN4 and HN12 cells were higher than that of the IHOK cells after 3 days of culture, suggesting that both the HN4 and HN12 cells were more resistant than the IHOK cells to the DFO-induced growth inhibition.

### *Morphologic appearance of organotypic cultures treated with DFO*

The 3D organotypic cultures of the control HaCaT and IHOK cells produced epithelial stratification with well-preserved morphologic differentiation and generally at least six layers with a distinct keratin layer showing good cellular polarity of differentiation (Fig. 2a). By contrast, the 1-mM DFO-treated HaCaT and IHOK cells produced only one or two cell layers with less keratinization and stratification than the untreated controls (Fig. 2b). The 3D organotypic cultures of the oral cancer cells (HN4 and HN12) revealed hyperchromatism and pleomorphism in the microsections, while the same culture treated with DFO showed less epithelial maturation and decreased epithelial thickness and surface keratinization than the control. Light microscopy revealed that the keratinocytes treated with 1 mM DFO showed severe growth retardation regardless of keratinocyte type and also displayed decreased keratinization and a reduced number of cell layers (Fig. 2b).

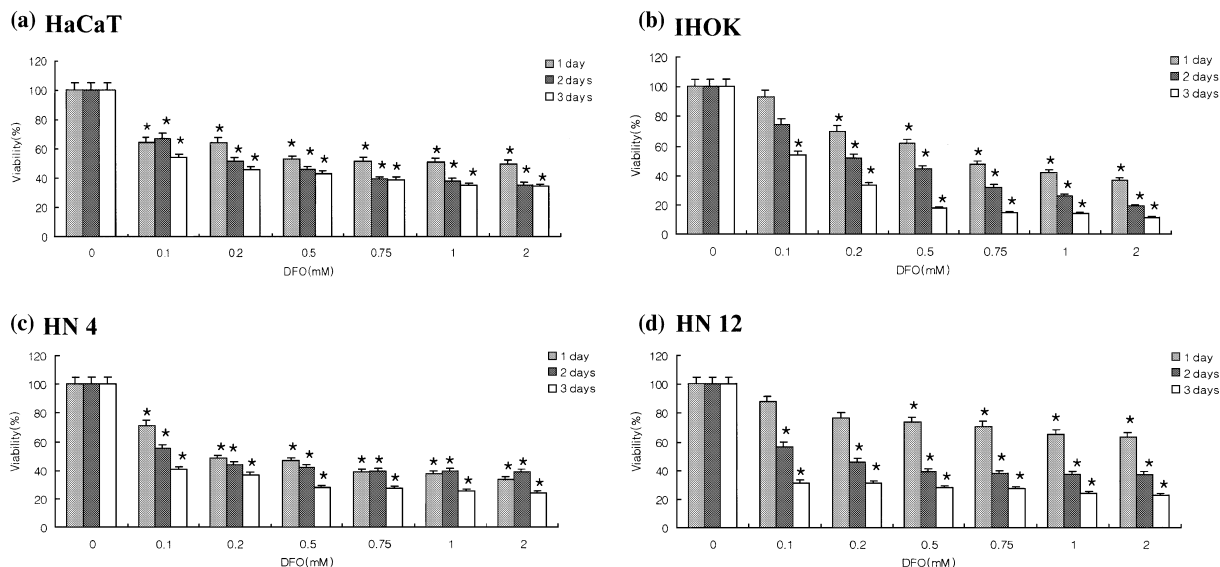


**Figure 1** Effects of DFO on cell viability on HaCaT (a), immortalized human oral keratinocyte (b), primary oral cancer (HN4) (c) and metastatic oral cancer (HN12) (d) cells as measured by MTT assay. Each points and bar represent a mean  $\pm$  SD. \* $P < 0.05$  versus controls.

**Table 1** DFO concentration (mM) required for 50% growth inhibition ( $IC_{50}$ ) in immortalized and malignant oral keratinocytes

Day	HaCaT	IHOK	HN4	HN12
1 day	0.94	0.99	0.72	1.78
2 days	0.73	0.64	0.66	0.66
3 days	0.65	0.43	0.50	0.49

#### Apoptosis induction by DFO treatment

Several assays were performed to determine if the growth inhibitory effect of DFO was attributable to the induction of apoptosis. First, the cell cycle analysis of keratinocytes treated with 1 mM DFO for 2 days demonstrated a distinct quantifiable population of cells with DNA content below the  $G_1$  phase level (a sub- $G_1$  peak), indicating apoptotic cells. As shown in Fig. 3a, the sub- $G_1$  fraction (hypodiploid DNA) increased in the DFO-treated group. Immortalized cells (IHOK and HaCaT) were more sensitive to DFO than were the cancer cells (HN4 and HN12), i.e. 1.0 mM DFO induced 13.25% of the IHOK cells but only 8.81% of the HN12 cells into the sub- $G_1$  peak.

Second, a DNA fragmentation assay using each type of keratinocytes treated with DFO for 48 h showed DNA laddering indicative of apoptosis (Fig. 3b). The DNA ladder formation was more evident in the IHOK cells than in the oral cancer cells.

Third, nuclear staining with DAPI, a fluorescent DNA-binding dye, demonstrated typical morphological features of apoptotic cells in all of the DFO-treated keratinocytes used in this study. The cells treated with 1 mM DFO displayed condensed and fragmented nuclei (Fig. 3c).

Lastly, flow cytometric analysis using Annexin V/PI double-staining revealed that the percentage of FITC-Annexin V-positive/PI-negative cells, which were apoptotic rather than necrotic, increased more than 10%

after 2 days of treatment with 1 mM DFO in IHOK cells (Fig. 3d). Collectively, these results indicate that DFO induced apoptosis in both the immortalized (IHOK and HaCaT) and malignant (HN4 and HN12) keratinocytes. Among the keratinocytes, the IHOK cells were more sensitive to apoptotic induction by DFO than that of oral cancer cells.

#### Western blot analysis for the intracellular levels of apoptosis-related proteins

We assessed the expression of apoptosis-related proteins, including p53, p21<sup>WAF1/CIP1</sup>, Bcl-2 and Bax by Western blot analysis (Fig. 4) to further characterize the cellular apoptosis induced by DFO. It is well known that p53 expression is essential for apoptosis caused by DNA damage (28). As shown in Fig. 4, p53 and p21<sup>WAF1/CIP1</sup> proteins increased more in the DFO-treated immortalized and malignant oral keratinocytes than in the controls.

The cytochrome *c*-initiated caspase cascade has been shown to be regulated by the Bcl-2 family of proteins. The balance between anti-apoptotic and pro-apoptotic Bcl-2 family members is critical in determining the susceptibility of cells to apoptosis signals (29). Therefore, this study aimed to examine the influence of DFO on the Bcl-2 family proteins and found that DFO downregulated the Bcl-2 protein, while it upregulated the Bax protein in both the immortalized and malignant oral keratinocytes.

#### Activation of caspase-3 and release of cytochrome *c* in iron chelator-induced apoptosis of immortalized and malignant oral keratinocytes

The caspase-3 activity is known to be increased during iron chelator-induced apoptosis in some cells (30, 31). In this study, the caspase-3 activities were examined in the keratinocytes undergoing DFO-induced apoptosis. IHOK and HN4 cells treated with 1.0 mM DFO showed

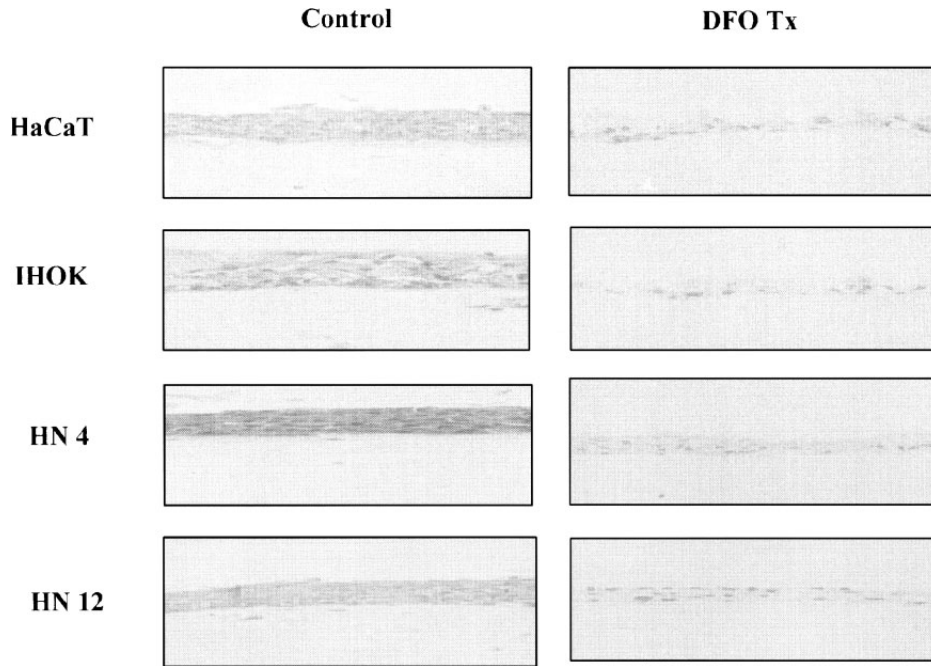


**Figure 2** Organotypic culture of immortalized and malignant oral keratinocytes cells treated with or without 1 mM DFO for 2 weeks (hematoxylin and eosin stain). (a) Control epithelial cells exhibiting usual stratification and multiple layers of cells ( $\times 200$ ). (b) Same cells treated with DFO. These cells showed poor stratification and less organized cell layers ( $\times 200$ ).

increased caspase-3-like activity for up to 48 h after DFO treatment (Fig. 5a). The activation and cleavage of caspase-3 tended to be time-dependent only in the IHOK cells (Fig. 5b,c). The cleaved forms of caspase-3 or caspase-8 were not detected in DFO-treated HN4 cells, but the levels of inactive forms of caspase-3 and caspase-8 decreased 24 h after DFO treatment. These results indicate that the DFO-induced apoptosis of immortalized and malignant oral keratinocytes is differentially regulated through the activation of caspase-3.

The level of cytosolic cytochrome *c* was examined using Western blot analysis because the release of cytochrome *c* from mitochondria is another cellular event associated with cell death (32). DFO-induced cytochrome *c* release into the cytosol appeared after 12 h in the IHOK cells and after 24 h in the HN4 cells (Fig. 5d). These results indicate that iron chelator-induced apoptosis of immortalized and malignant oral keratinocytes is dependent on cytochrome *c* release from mitochondria.

## Discussion

Considering the potential of iron chelators to inhibit the proliferation of tumor cells, we investigated the influence of DFO on the proliferation, cell cycle and apoptosis of HPV-IHOK, skin immortalized keratinocytes (HaCaT), primary oral cancer cells (HN4) and metastatic oral cancer cells (HN12) *in vitro* to determine the molecular and biological basis for the anticancer effects of iron chelators in oral cancer.

We found that DFO had growth inhibitory effects on human oral immortalized and malignant keratinocyte

(Fig. 1). These effects were relatively dose-dependent and displayed maximal inhibition in the 2 mM DFO treatment groups after 3 days. The immortalized keratinocytes (IHOK, oral and HaCaT, skin) showed greater DFO-induced growth inhibition than did the oral malignant keratinocytes (HN4 and HN12). The anti-proliferative effects of iron chelators that we observed with the IHOK and oral cancer cells are in accordance with the results of other studies showing that iron chelators inhibit DNA synthesis in proliferating cells, such as leukemia, neuroblastoma, melanoma, hepatoma, human cervical carcinoma and Kaposi's sarcoma cells (18–23).

Desferrioxamine also dose-dependently inhibited the *in vitro* proliferation of cervical cancer cells; the  $IC_{50}$  values for DFO exposure ranged from 0.054 mM after 2 days for SiHa cells to 0.042 mM after 2 days for HeLa cells (23). In contrast, it was demonstrated that the  $IC_{50}$  values of our IHOK and oral cancer cell lines for DFO were from 0.64 to 0.73 mM after 2 days of culture. This means that the IHOK and oral cancer cells displayed a 12- to 17-fold resistance to DFO compared with cervical cancer cells. Thus, higher concentrations of DFO are required to inhibit the proliferation of oral cancer cells compared with cervical cancer cells.

As oral mucosae are composed of stratified squamous epithelium, we believe that a 3D culture method could be an adequate model for investigating the pharmacological influence of some drugs on the morphology, functions and differentiation of keratinocytes *in vitro* (27). According to our results, in the 3D organotypic culture, the immortalized and malignant keratinocytes treated with DFO showed less epithelial maturation

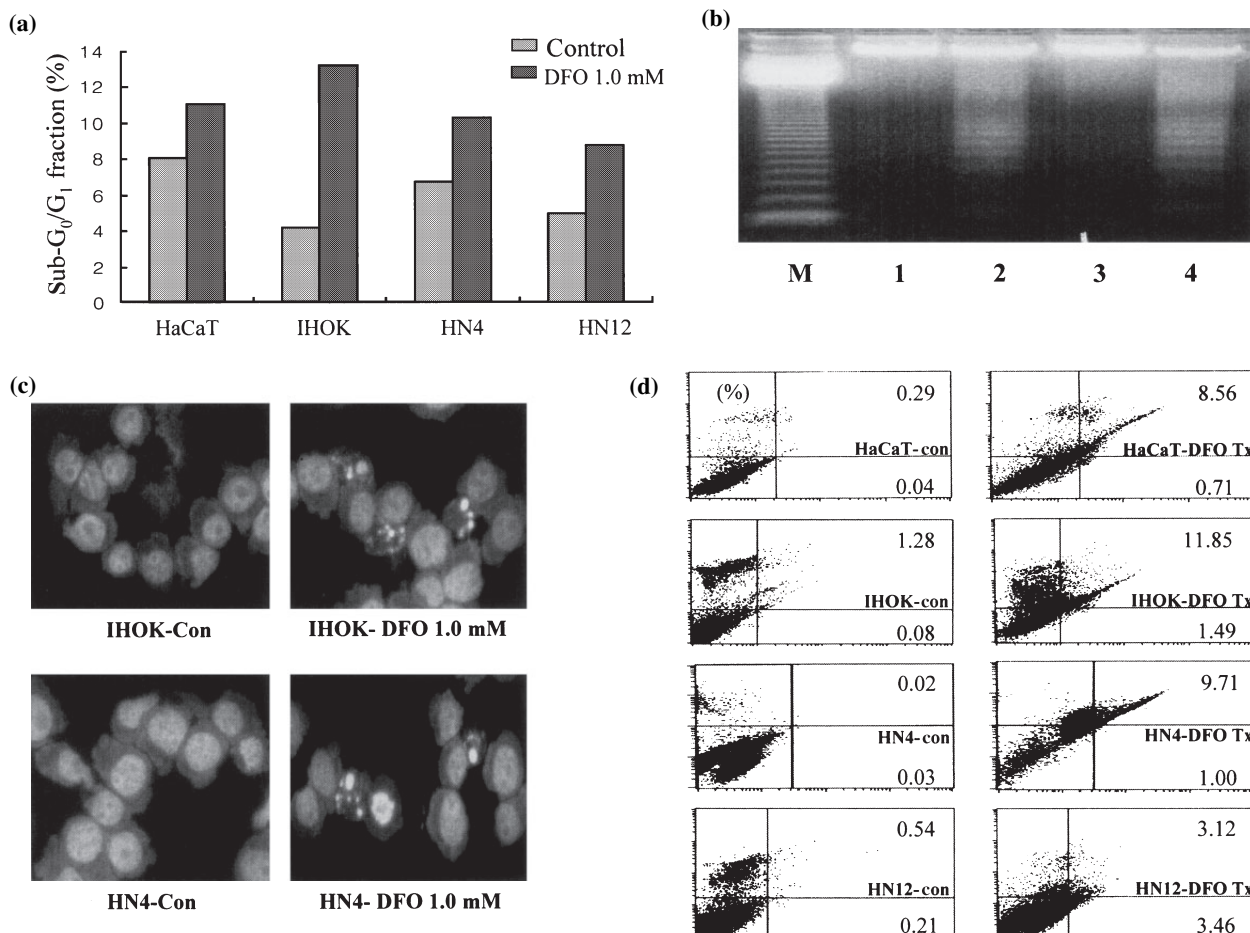


**Figure 3** Confirmation of DFO induced apoptosis treatment in immortalized and malignant oral keratinocytes by cell cycle analysis (a), DNA laddering (b), DAPI staining (c), Annexin V-PI flow cytometry (d). (a) Representative sub-G<sub>1</sub> phase of cell cycle distribution in the presence and absence of 1 mM DFO for 2 days. The cells were analyzed for DNA content by staining with propidium iodide followed by FACS analysis as described in materials and methods. (b) DNA fragmentation was analyzed by 2% agarose gel electrophoresis. (c) Nuclear DAPI staining. Cells were treated as described in Fig. 2 and DAPI stained nuclei were visualized under a fluorescence microscope (×200). (d) Representative Annexin V-PI flow cytometric analysis. Cells were incubated with 1 mM DFO for 2 days. And then they were stained with FITC-conjugated Annexin V and PI for flow cytometry.

and displayed decreased epithelial thickness and surface keratinization compared with the control cells and DFO resulted in the severe inhibition of proliferation and differentiation in all of the keratinocytes used in this study.

Few data have been published concerning the molecular basis of the inhibitory effects of iron chelators on proliferation. However, it has been shown that iron depletion arrests human neuroblastoma cells in late G<sub>1</sub> phase of the cell cycle (33) and breast cancer cells at the G<sub>1</sub>/S transition (34) and that this effect is mediated through the inhibition of the expression of cyclin and/or the induction of cyclin-dependent kinase complexes, such as cyclin D1/cdk4 (35). Cell cycle studies have shown that iron chelator-treated cells are arrested in different phases of the cell cycle depending upon the cell type, the chelator concentration and the time of exposure to the chelator. Moreover, several authors have reported that iron chelators induce apoptosis in proliferating cells, such as activated T lymphocytes, promyelocytic HL60 cells and murine lymphoma cells (35, 36).

We primarily focused on determining whether DFO possesses the potential to induce cellular apoptosis in immortalized and malignant oral keratinocytes in order to study the mechanism of the anti-proliferative activity of DFO. We have shown that DFO, at cytotoxic micromolar concentrations, can trigger apoptosis in IHOK and oral cancer cells. This notion is based on the following evidence: (i) cell cycle analysis showed that the immortalized and malignant oral keratinocytes displayed increased numbers of hypodiploid nuclei after DFO treatment (Fig. 3a), (ii) IHOK and oral cancer cells underwent internucleosomal DNA fragmentation (Fig. 3b) and morphological nuclear changes characteristic of apoptosis (Fig. 3c) and (iii) FITC-Annexin V and PI double-staining revealed that the apoptotic cell population with FITC-Annexin V<sup>+</sup>/PI<sup>-</sup> increased after the exposure to DFO in immortalized and malignant oral keratinocytes (Fig. 3d).

To investigate the mechanisms by which DFO inhibits the cell cycle progression of immortalized and malignant oral keratinocytes and to identify the proteins that are

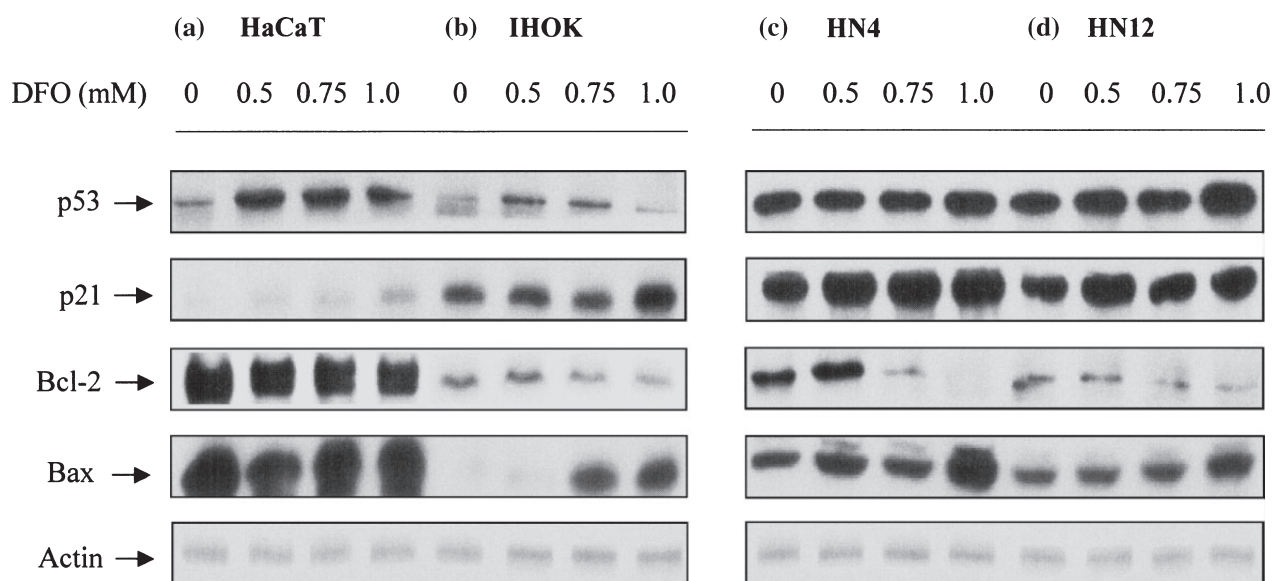


**Figure 4** Western blot analysis of cell cycle regulatory protein expression of p53, p21, Bax and Bcl-2 in HaCaT (a), IHOK (b), HN4 (c) and HN12 (d) cells cultured without or with different concentration of DFO for 2 days. The protein fraction was extracted, electrophoresed, transferred to membrane and blotted with respective antibodies. These data are representative of three independent experiments.

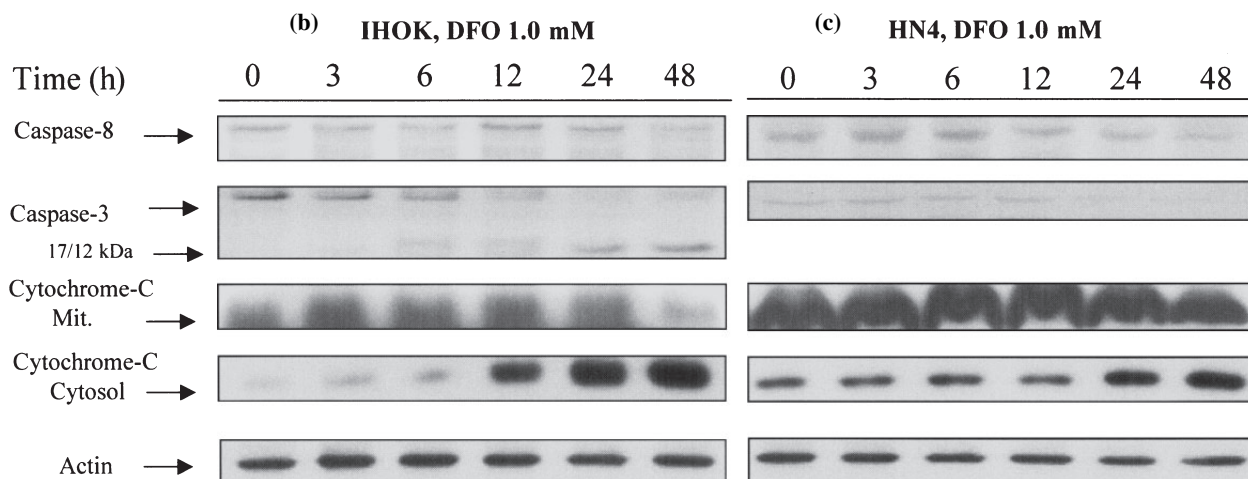
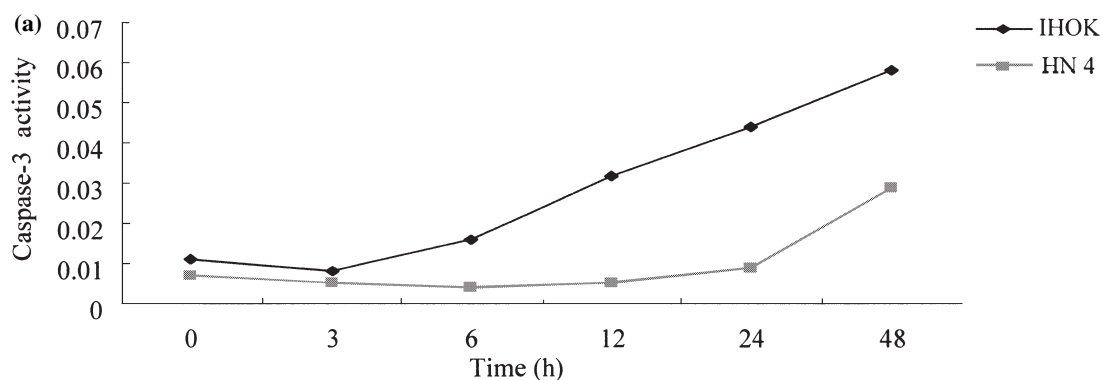


**Figure 5** Activation of caspase and cytochrome *c* during iron deprivation-induced apoptosis of immortalized and malignant oral keratinocytes. The enzymatic activity of capase-3 (a) was determined by incubation of the lysate with colorimetric substrates, AC-DEAD-pNA. Western blot analysis of capase-3 and cytochrome *c* proteins in immortalized (b) and malignant oral keratinocytes (c). Cells were cultured with 1 mM DFO for different incubation periods and then subjected to the procedure described in the legend to materials and methods. The data shown are representative of three independent experiments.

involved in the process, cell cycle regulation studies were performed. DNA damage activates p21<sup>WAF1/CIP1</sup> transcription in a p53-dependent manner in human fibroblasts and epithelial cells (37) and it has also been demonstrated that p53 induces apoptosis by means of a direct signaling pathway (38). The overexpression of p53 results in cell cycle arrest via the activation of p21<sup>WAF1/CIP1</sup>, which leads to the inactivation of cyclin-dependent kinases (38). In the present study, the levels of p53 and p21<sup>WAF1/CIP1</sup> increased in the presence of DFO in IHOK and oral cancer cells, whereas the level of Rb did not change, compared with levels in the control (data not shown). These results indicate that p53 and p21<sup>WAF1/CIP1</sup> expression may affect the apoptosis pathway in immortalized keratinocytes and malignant oral keratinocytes treated with DFO.

The Bcl-2 oncoprotein and other related proteins play an important role in determining whether cells undergo necrosis or apoptosis. The increased expression of Bax can promote apoptosis by suppressing the activity of Bcl-2 (39). On the other hand, the Bcl-2 protein is recognized as a main negative regulator of apoptosis and acts upstream of caspase-3 to prevent apoptosis. We found that DFO induced apoptosis through the down-regulation of the Bcl-2 protein and the upregulation of Bax, p53 and p21<sup>WAF1/CIP1</sup>. These processes may comprise the main molecular mechanisms for the apoptosis of immortalized keratinocytes and malignant oral keratinocytes treated with DFO.

Caspase-8 and caspase-3 are known initiators for the cell death-receptor signal pathways, which are activated by many chemotherapeutic drugs (40). Our results demonstrate that the immortalized keratinocytes (HaCaT and IHOK) treated with DFO activated the caspase-3 mediated apoptotic pathways, which resulted in the augmentation of apoptotic cell death.

There are two distinct pathways that initiate apoptosis, designated as mitochondrial and death-receptor pathways (41). The intrinsic pathway, or mitochondrial pathway, is triggered by the release of cytochrome *c* from mitochondria. In our study, DFO effectively promoted the release of cytochrome *c* into the cytosol in IHOK and oral cancer cells, which consequently activated caspase-3, while caspase-8 was unaffected in the IHOK and oral cancer cells. These data demonstrate that DFO-induced apoptosis can be differentially regulated through the mitochondrial-mediated pathways in keratinocytes.

Meanwhile, the effect of iron chelator is not just restricted on chelating cellular iron pool, but is also involved in modulating oxidative stresses induced by several environmental stresses including iron overload, (42). A chemically induced 'hypoxic' state is induced by DFO resulting in an upregulation or stabilization of hypoxia-inducible factor-1 $\alpha$  (HIF-1 $\alpha$ ) (42, 43). HIF-1 $\alpha$  is a nuclear protein induced during hypoxia essential for transcriptional activation of hypoxia-inducible genes such as erythropoietin, glucose transporters, glycolytic enzymes, vascular endothelial growth factor (VEGF) and other genes whose protein products increase oxygen delivery or facilitate metabolic adaptation to hypoxia (44). More recently, hypoxia-inducible factor-1 (HIF-1),

a protein which is over accumulated in the state of hypoxia, is known to play an important role in leukemic cell differentiation (45). Thus, the question whether DFO induces HIF-1 in oral cancer cells or otherwise, whether transfection of HIF-1 induces differentiation still remains for further study in immortalized and malignant keratinocytes.

In summary, DFO treatment in immortalized (IHOK and HaCaT) and oral malignant (HN4 and HN12) keratinocytes markedly inhibited the proliferation of epithelial cells and resulted in the retardation of cell cycle progression via the mitochondrial-mediated apoptosis pathway. The immortalized keratinocytes were more sensitive to DFO treatment than the oral malignant keratinocytes in the expression of cell cycle regulatory proteins and apoptosis markers.

## References

1. Marcus B, Arenberg D, Lee J et al. Prognostic factors in oral cavity and oropharyngeal squamous cell carcinoma. *Cancer* 2004; **15**: 2779–87.
2. Kok TC, Van der Gaast A, Dees J et al. Cisplatin and etoposide in oesophageal cancer: a phase study. *Br J Cancer* 1996; **74**: 980–4.
3. McCann J. Texas center studies research alternative treatments. *J Natl Cancer Inst* 1997; **89**: 1485–6.
4. Cassileth BR, Chapman CC. Alternative and complementary cancer therapies. *Cancer* 1996; **77**: 1026–34.
5. Gutteridge JM. Iron and oxygen: a biologically damaging mixture. *Acta Paediatr Scand Suppl* 1989; **361**: 78–85.
6. Stevens RG. Iron and the risk of cancer. *Med Oncol Tumor Pharmacother* 1990; **7**: 177–81.
7. Hann HW, Stahlhut MW, Hann CL. Effect of iron and desferoxamine on cell growth and in vitro ferritin synthesis in human hepatoma cell lines. *Hepatology* 1990; **11**: 566–9.
8. McCormack M, Nias AH, Smith E. Chronic anaemia, hyperbaric oxygen and tumour radiosensitivity. *Br J Radiol* 1990; **63**: 752–9.
9. Siegert CP, Bumann D, Trepkau HD, Schadwinkel B, Baretton D. Influence of dietary iron overload on cell proliferation and intestinal tumorigenesis in mice. *Cancer Lett* 1992; **65**: 245–9.
10. Damber L, Larsson LG. Combined effects of mining and smoking in the causation of lung carcinoma. A case-control study in northern Sweden. *Acta Radiol Oncol* 1982; **21**: 305–13.
11. Edling C. Lung cancer and smoking in a group of iron ore miners. *Am J Ind Med* 1982; **3**: 191–9.
12. Mandishona E, MacPhail AP, Gordeuk VR et al. Dietary iron overloads a risk factor for hepatocellular carcinoma in black Africans. *Hepatology* 1998; **27**: 1563–66.
13. Van Asperen IA, Feskens EJ, Bowles CH, Kromhout D. Body iron stores and mortality due to cancer and ischemic heart disease: a 17-year follow-up study of elderly men and women. *Int J Epidemiol* 1995; **24**: 665–70.
14. Gorodetsky R, Sheskin J, Weinreb A. Iron, copper, and zinc concentrations in normal skin and in various nonmalignant and malignant lesions. *Int J Dermatol* 1986; **25**: 440–4.
15. Pilch J, Gierek T, Laskawiec J, Grzybek H. The use of X-ray microanalysis and transmission microscopy in studies of the chemical composition and ultrastructure of

- the microregions of precancerous tissues of the larynx. *Otolaryngol Pol* 1996; **50**: 471–8.
16. Weinberg ED. The role of iron in cancer. *Eur J Cancer Prev* 1996; **5**: 19–36.
  17. Donfrancesco A, Deb G, Dominici C, Pileggi D, Castello MA, Helson L. Effects of single course of deferoxamine in neuroblastoma patients. *Cancer Res* 1990; **50**: 4929–30.
  18. Haq RU, Werely JP, Chitambar CR. Induction of apoptosis by iron deprivation in human leukemic CCRF-CEM cells. *Exp Hematol* 1995; **23**: 428–32.
  19. Fukuchi K, Tomoyasu S, Tsuruoka N, Gomi K. Iron deprivation-induced apoptosis in HL-60 cells. *FEBS Lett* 1994; **350**: 139–42.
  20. Becton DL, Bryles P. Deferoxamine inhibition of human neuroblastoma viability and proliferation. *Cancer Res* 1988; **48**: 7189–92.
  21. Hann HW, Stahlhut MW, Hann CL. Effect of iron and desferoxamine on cell growth and *in vitro* ferritin synthesis in human hepatoma cell lines. *Hepatology* 1990; **11**: 566–9.
  22. Simonart T, Degraef C, Andrei G et al. Iron chelators inhibit the growth and induce the apoptosis of Kaposi's sarcoma cells and of their putative endothelial precursors. *J Invest Dermatol* 2000; **115**: 893–900.
  23. Simonart T, Boelaert JR, Mosselmans R et al. Anti-proliferative and apoptotic effects of iron chelators on human cervical carcinoma cells. *Gynecol Oncol* 2002; **85**: 95–102.
  24. Oda D, Bigler L, Lee P, Blanton R. HPV immortalization of human oral epithelial cells: a model for carcinogenesis. *Exp Cell Res* 1996; **226**: 164–9.
  25. Boukamp P, Petrussevska RT, Breitkreutz D, Hornug J, Markham A, Fusenig NE. Normal keratinization in a spontaneously immortalized aneuploid human keratinocyte cell line. *J Cell Biol* 1988; **106**: 761–71.
  26. Cardinali MH, Pietraszkiewicz JF, Robbins KC. Tyrosine phosphorylation as a marker for aberrantly regulated growth-promoting pathways in cell lines derived from head and neck malignancies. *Int J Cancer* 1995; **61**: 98–103.
  27. Chung JH, Cho KH, Lee DY et al. Human oral buccal mucosa reconstructed on dermal substrates: a model for oral epithelial differentiation. *Arch Dermatol Res* 1997; **289**: 677–85.
  28. Lowe SW, Schmitt EM, Smith SW, Osborne BA, Jacks T. p53 is required for radiation-induced apoptosis in mouse thymocytes. *Nature (London)* 1992; **362**: 847–49.
  29. Oh Sh, Lee BH, Lim SC. Cadmium induces apoptotic cell death in WI 38 cells via caspase-dependent Bid cleavage and calpain-mediated mitochondrial Bax cleavage by Bcl-2-independent pathway. *Biochem Pharmacol* 2004; **68**: 1845–55.
  30. Georgiou NA, van der Bruggen T, Oudshoorn M, Hider RC, Marx JJ, van Asbeck BS. Human immunodeficiency virus type 1 replication inhibition by the bidentate iron chelators CP502 and CP511 is caused by proliferation inhibition and the onset of apoptosis. *Eur J Clin Invest* 2002; **1**(32 Suppl):91–6.
  31. Ido Y, Muto N, Inada A et al. Induction of apoptosis by hinokitiol, a potent iron chelator, in teratocarcinoma F9 cells is mediated through the activation of caspase-3. *Cell Prolif* 1999; **32**: 63–73.
  32. Yang J, Liu X, Bhalla K et al. Prevention of apoptosis by Bcl-2: release of cytochrome *c* from mitochondria blocked. *Science* 1997; **275**: 1129–32.
  33. Brodie C, Siriwardana C, Lucas J et al.. Neuroblastoma sensitivity to growth inhibition by desferioxamine: evidence for block in G1 phase of the cell cycle. *Cancer Res* 1993; **53**: 3969–75.
  34. Kulp KS, Green SL, Vulliet PR. Iron deprivation inhibits cyclin-dependent kinase activity and decreases cyclin D/CDK4 protein levels in asynchronous MDA-MB-453 human breast cancer cells. *Exp Cell Res* 1996; **229**: 60–8.
  35. Hileti D, Panayiotidis P, Hoffbrand AV. Iron chelators induce apoptosis in proliferating cells. *Br J Haematol* 1995; **89**: 181–7.
  36. Kovar J, Stunz LL, Stewart BC, Kriegerbeckova K, Ashman RF, Kemp JD. Direct evidence that iron deprivation induce apoptosis in murine lymphoma 38C13. *Pathobiology* 1997; **65**: 61–8.
  37. Dulic V, Kaufmann WK, Wilson SJ et al. p53-dependent inhibition of cyclin-dependent kinase activities in human fibroblasts during radiation-induced G1 arrest. *Cell* 1994; **76**: 1013–23.
  38. Clarke AR, Purdie CA, Harrison DJ et al. Thymocyte apoptosis induced by p53 dependent and independent pathways. *Nature (London)* 1993; **362**: 849–52.
  39. Reed JC. Dysregulation of apoptosis in cancer. *J Clin Oncol* 1999; **17**: 2941–53.
  40. Sun XM, MacFarlane M, Zhuang J, Wolf BB, Green DR, Cohen GM. Distinct caspase cascades are initiated in receptor mediated and chemical induced apoptosis. *J Biol Chem* 1999; **274**: 5053–60.
  41. Chang HY, Yang X. Proteases for cell suicide: functions and regulations of caspases. *Microbiol Mol Biol Rev* 2000; **64**: 821–46.
  42. Britton RS, Leicester KL, Bacon BR. Iron toxicity and chelation therapy. *Int J Hematol* 2002; **76**: 219–28.
  43. Zaman K, Ryu H, Hall D et al. Protection from oxidative stress-induced apoptosis in cortical neuronal cultures by iron chelators is associated with enhanced DNA binding of hypoxia-inducible factor-1 and ATF-1/CREB and increased expression of glycolytic enzymes, p21(waf1/cip1), and erythropoietin. *J Neurosci* 1999; **19**: 9821–30.
  44. Yang YT, Ju TC, Yang DI. Induction of hypoxia inducible factor-1 attenuates metabolic insults induced by 3-nitropropionic acid in rat C6 glioma cells. *J Neurochem* 2005; **93**: 513–25.
  45. Jiang Y, Xue ZH, Shen WZ et al. Desferrioxamine induces leukemic cell differentiation potentially by hypoxia-inducible factor-1 alpha that augments transcriptional activity of CCAAT/enhancer-binding protein-alpha. *Leukemia* 2005; **19**: 1239–47.

This document is a scanned copy of a printed document. No warranty is given about the accuracy of the copy. Users should refer to the original published version of the material.